Case Studies of Vibrations in Structures

Jorge Miguel Proença* – Fernando Branco*

*ICIST/IST
Instituto de Engenharia de Estruturas, Território e Construção do Instituto Superior Técnico
Av. Rovisco Pais, 1049-001, Lisbon, Portugal
jmiguel@civil.ist.utl.pt
fbranco@civil.ist.utl.pt

ABSTRACT: *Mechanical vibrations in structures can lead to a wide variety of detrimental effects, ranging from human health and comfort impairment, to possible damage, both to sensitive equipment and structural components. In other situations, ambient vibrations can be used beneficially to extract valuable information about the structural behaviour, through the identification of mode shapes and frequencies. Modal identification results can subsequently be used as a part of the vibration reduction methodologies. The analytical background required by each of these two situations is presented. Some case studies that characterize the experience gathered by ICIST/IST over the last 15 years are also presented.*

RÉSUMÉ: *Les vibrations mécaniques en structures peuvent mener à une grande variété d'effets néfastes, qui s'étendent de l'affaiblissement de la santé humaine et du confort, aux dommages aux équipements et structures. En parallèle, les vibrations ambiantes peuvent être employées avantageusement pour extraire des informations sur le comportement de la structure, notamment les modes de vibration et les correspondantes fréquences. Les résultats de l'identification modale peuvent être employés comme outils des techniques de réduction des vibrations. Le fondement analytique exigé par chacune des deux situations est présenté. Quelques études de cas, qui représentent l'expérience recueillie par l'ICIST/IST au cours des dernières 15 années, sont également présentées.*

KEYWORDS: *modal identification, mechanical vibration, modal analysis, damping, vibration isolation, bridges*

MOTS-CLÉ: *identification modale, vibrations mécaniques, analyse modale, amortissement, isolation de vibrations, ponts a haubans*

Proença, JMSFM; Branco, FAB - Case studies of vibrations in structures, Revue Européenne de Génie Civil, Vol. 9/1-2, pp.159-186, Lavoisier, 2005.

1. Introduction

In the last 15 years, ICIST/IST (Technical University of Lisbon) has been asked to study mechanical vibration effects on a growing number of structures in Portugal. The increase in the diversity, quantity and quality of studies of vibration effects on structures has mostly resulted from the development and generalization of adapted vibration transducers, enhanced by the possibilities of digitally processing vibration records.

Vibration studies can range from modal identification – under ambient, transient or forced load conditions – to vibration problems.

Vibration problems are usually associated to damage in sensitive equipments, nuisance to human health and comfort, and damage in structural components.

Modal identification studies – aimed at the identification of modal frequencies, mode shapes and damping ratios – serve to validate or to enhance the exactness of numerical models or to assess the extent of alleged structural damage. These studies can also be used beneficially as a part of the vibration reduction methodologies.

Vibration problems generally require vibration characterization in terms of peak values, preferred vibration indicators, frequency content and identification of the predominant sources and vibration transmission paths.

The present paper exemplifies the relevant experience gathered along the last 15 years by ICIST/IST, firstly by the presentation of the analytical background in each of the applicable vibration studies, and finally by the presentation of representative case studies of mechanical vibrations in structures.

2. Analytical Background

2.1 Generalities

Mechanical vibration effects studies on structures can be subdivided into modal identification and vibration problems.

Due to the difficulties of accurately controlling the excitation imparted on the structure, modal identification of civil engineering structures has evolved into so-called *output only methods* (Ventura 2000), of which the presented Basic Frequency Domain (BFD) method is an example.

Mechanical vibrations in structures can also cause problems to human health and comfort, to the operation of sensitive equipment and to the integrity of the structure itself.

The analytical background required by modal identification and vibration problem assessment is substantially different. This difference has led to the following two subsections.

2.2 Modal Identification

In MDOF (multi degree of freedom) linear elastic structural systems, the force-to-displacement FRF (Frequency Response Function), $\boldsymbol{H(\omega)}$, can be expressed in terms of the structural matrices $\boldsymbol{M}$ (mass), $\boldsymbol{C}$ (viscous damping) and $\boldsymbol{K}$ (stiffness):

$$\boldsymbol{H}(\omega) = \left(-\omega^2 \boldsymbol{M} + i\omega\boldsymbol{C} + \boldsymbol{K}\right)^{-1} \qquad [1]$$

in which ω stands for the forcing frequency (angular).

This (matrix) function can, alternatively, be derived in terms of the mass-normalised modal shapes $\boldsymbol{\Phi}$, frequencies p and viscous damping ratios ζ,:

$$\boldsymbol{H}(\omega) = \boldsymbol{\Phi}\left[-\omega^2 \boldsymbol{I} + i\omega[2\xi p] + \left[p^2\right]\right]^{-1} \boldsymbol{\Phi}^T \qquad [2]$$

where $[2\zeta p]$ and $[p^2]$ are diagonal matrices which are expressed in terms of the modal (angular) frequencies p and modal viscous damping ratios ζ ($\boldsymbol{I}$ stands for the identity matrix). Each of the individual terms of this FRF can then be explicitly obtained by:

$$H_{mn}(\omega) = \sum_{k=1}^{N} \frac{\Phi_{mk}\Phi_{nk}}{-\omega^2 + i2\xi_k p_k \omega + p_k^2} \qquad [3]$$

The generic term $Hmn(\omega)$ is a complex function that describes the amplitude and phase lag for the steady-state displacement component at the m^{th} DOF when a harmonic unitary excitation force is applied at the n^{th} DOF. The former expression shows that the amplitude of the response results from the superposition of the individual mode effects, in which the contribution of each mode k mainly depends on the proximity between the excitation frequency ω and the modal frequency p_k and, also, on the displacement ordinates for the modal shape $\boldsymbol{\phi_k}$ at the DOFs where the excitation is applied and where the response is measured. In the general case where these two latter modal shape coefficients are both different from zero, the corresponding Hmn term should exhibit a clear peak at the vicinity of each of the modal frequencies.

Whenever the excitation frequency ω is in the vicinity of a given modal frequency p_k, the corresponding modal term contribution clearly dominates the former expression, and the corresponding FRF term can then be approximated by the resonant mode contribution, or:

$$H_{mn}(\omega) \approx \frac{\Phi_{mk}\,\Phi_{nk}}{-\omega^2 + i2\zeta_k p_k \omega + p_k{}^2} \quad [4]$$

Another relevant transfer function is the force-to-acceleration FRF, sometimes referred (Ewins 1986) to as *Inertance*, which can be derived from $\boldsymbol{H}(\omega)$ through:

$$\boldsymbol{I}(\omega) = \omega^2 \boldsymbol{H}(\omega) \quad [5]$$

Under the former circumstances (single-mode contribution) the absolute square value of the individual *mn* term of the Inertance matrix can be approximated by:

$$\left|I_{mn}(\omega)\right|^2 \approx \frac{\omega^4 \left(\Phi_{mk}\Phi_{nk}\right)^2}{p_k^4\left((1-(\omega/p_k)^2)^2 + (2\xi_k(\omega/p_k))^2\right)} \quad [6]$$

In the general case of the so-called "ambient vibration", in which the structural vibration is due to a multitude of causes (e. g.: wind, traffic in the vicinity, etc.) the excitation can be approximated by a broadband ergodic stationary stochastic process, commonly referred to as *white noise* process. Under these conditions the response (displacement) auto power spectral density function $\boldsymbol{S}^{qq}(\omega)$ is proportional to the force-to-displacement FRF:

$$\boldsymbol{S}^{qq}(\omega) \propto \boldsymbol{H}(\omega) \times \boldsymbol{H}(\omega)^{*T} \quad [7]$$

where the (*) and (^{T}) symbols represent, respectively, the complex conjugate and transpose matrices.

The former equation shows one of the most relevant results in ambient vibration modal identification: independently of the excitation characteristics and source (provided that the *white noise* assumption is acceptable), the response auto power spectral density closely follows the shape of the FRF, presenting peaks coincident with the modal frequencies p_k and having a general shape determined by the relevant modal shape coefficients (ϕ_{mk} and ϕ_{nk}) and modal damping ratio ζ_k.

In the more practical case of force-to-acceleration FRF (Inertance), the diagonal *mm* term of the acceleration auto power spectral density, in the vicinity of the $k^{th.}$ modal frequency, follows:

$$S_{mm}^{aa}(\omega) \approx \frac{A\,\omega^4}{(1-(\omega/p_k)^2)^2 + (2\xi_k\omega/p_k)^2} \quad [8]$$

where A is a variable which depends on the excitation intensity and on the modal shape coefficient ϕ_{mk}. This equation can be used to estimate the modal frequencies (which correspond to peaks in the acceleration auto power spectral density) and, through curve fitting, modal damping ratios can also be assessed.

Maintaining the same *white noise* assumption, modal coefficients can be estimated by the so-called Basic Frequency Domain Method (Ventura 2000). This method is based on the following equation

$$\frac{\ddot{Y}_a(p_k)}{\ddot{Y}_b(p_k)} \approx \frac{p_k^2 \Phi_{ak} \cdot H_k(\omega) \cdot Q_k(\omega)}{p_k^2 \Phi_{bk} \cdot H_k(\omega) \cdot Q_k(\omega)} \approx \frac{\Phi_{ak}}{\Phi_{bk}} \qquad [9]$$

where:

$\ddot{Y}_a(p_k)$ and $\ddot{Y}_b(p_k)$ are the Fourier transforms of the ambient vibration acceleration records at degrees of freedom *a* and *b*, at frequency p_k, and,

Φ_{ak} and Φ_{bk} represent the $k^{th.}$ modal shape coefficients at DOFs *a* and *b*,

p_k is the (angular) modal frequency of mode *k*,

$Q_k(\omega)$ is the Fourier transform of the $k^{th.}$ mode modal force,

$H_k(\omega)$ is the (SDOF) force-to-displacement transfer function for mode *k*.

The former equation shows that the $k^{th.}$ modal shape coefficients at degrees of freedom *a* and *b* can be assessed through the computation of the correspondent ratio of the acceleration Fourier transform ordinates for modal frequency ω_k. This method requires that the supposedly ambient vibration acceleration records at degrees of freedom *a* and *b* are synchronous.

2.3 Mechanical Vibration Effects

2.3.1 *Mechanical Vibration Effects on Human Health and Comfort*

Human perception of mechanical vibrations, and their consequence to the health and comfort issues, depends on a multitude of factors, such as: vibration amplitude, frequency range, duration, predominant component and time of day.

When faced with the human health and comfort issues the application of standard DIN 4150, Part 2 (DIN 1975) has been considered. For the simplified case of harmonic vibrations, DIN 4150-2 (DIN 1975) and DIN 45669 (DIN 1995) define a perceptibility factor (KB factor), which empirically reflects the human perception of mechanical vibrations. In the same case of harmonic vibrations the KB factor can independently be determined for three possible measuring variables (*a*-acceleration; *v* – velocity; and *s* – displacement) according to:

$$KB = a\frac{\gamma_a}{\sqrt{1+\left(\frac{f}{f_0}\right)^2}}\ ; \qquad KB = v\frac{\gamma_v f}{\sqrt{1+\left(\frac{f}{f_0}\right)^2}}\ ; \qquad KB = s\frac{\gamma_s f^2}{\sqrt{1+\left(\frac{f}{f_0}\right)^2}} \qquad [10]$$

in which γ_a, γ_v and γ_s are empirically calibrated parameters, f is the vibration frequency, and f_0 is the threshold frequency above which human vibration perceptibility is more acute.

Vibration amplitude (a, v and s) can, alternatively, be defined in terms of its effective value, in which case the former perceptibility parameters are also termed effective. For the case of velocity the KB factor can be defined in

$$KB = v_{eff} \frac{\gamma_{v,eff}\ f}{\sqrt{1+\left(\dfrac{f}{f_0}\right)^2}} \qquad [11]$$

DIN 4150-2 (DIN 1975) considers that $\gamma_{v,eff}$=0.18 mm^{-1}s^2 and f_0=5.6 Hz. These values lead to the human isoperceptibility curves shown in figure 1 for effective velocity measurements and harmonic vibrations.

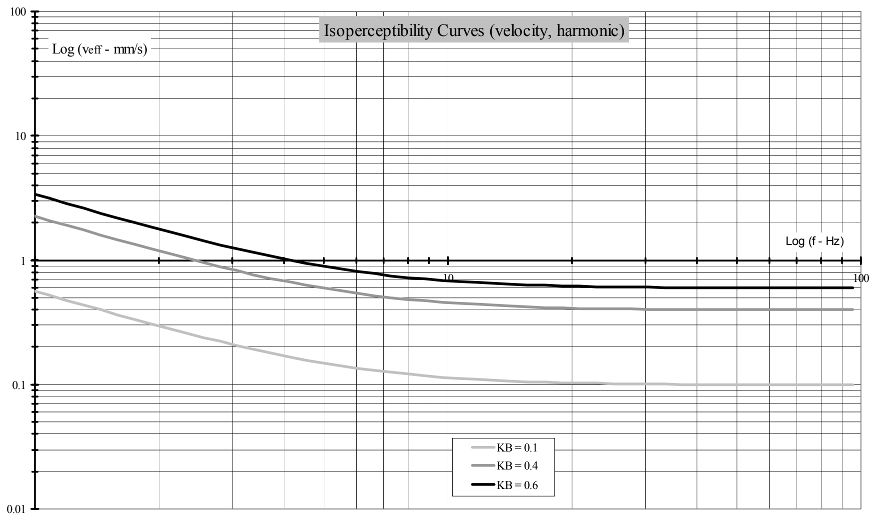

Figure 1. *Human isoperceptibility curves*

In practical situations, where the vibration is seldom harmonic, DIN 4150-2 (DIN 1975) suggest that the mechanical vibrations should be filtered by a human perceptibility filter (KB filter) that accounts for the different human susceptibility to the various harmonic components. KB filter is a lowpass filter, cut-off at 80 Hz, with a gradual attenuation of components below 20 Hz to 1 Hz. The KB-filtered velocity v_{KB} can then be defined as the convolution ($*$) of the vibration velocity with a KB filtering function w_{KB}.

$$v_{KB}(t) = \int_0^t v(t) \cdot w_{KB}(t-\tau)d\tau = v(t) * w_{KB}(t) \quad [12]$$

The KB factor is taken as the maximum value of the effective, KB-filtered, velocity signal. This KB factor is then compared with permissible values, taking into account the nature of the events (steady state or transient vibrations), the type of human use in the building (critical work areas, dwellings, offices and industry) and the period (day or night).

2.3.2 *Mechanical Vibration Effects on Sensitive Equipment*

Mechanical vibrations can also have detrimental effects on the operation of particularly sensitive equipment. This is the case of the so-called *advanced technology facilities*, such as microelectronics production (e. g.: semiconductor production) and nanotechnology research facilities, in which the mechanical vibration levels are increasingly important to the site selection, at the early investment stage, and to the quality and productivity, at the operation stage.

The sources of mechanical vibrations in a semiconductor fabrication facility can be classified, as to their source, according to the following list:

- External sources – transmitted through the ground supporting the structure. These external sources are naturally site-dependent and can consist of road traffic, train passages and other external activities. They are inherently random in nature and usually composed of stationary and transient components.
- Internal sources – due to constant speed rotating equipment (almost periodic excitation), footfall, AVAC and other fluid transmission pipes (random) and low-frequency airborne acoustic noise.

The external sources are determinant for the selection of semiconductor production sites in what are generally referred to as *greenfield site assessment studies*.

For two decades, researchers and industry have been working together to set the standards for the evaluation of mechanical vibration effects in extremely sensitive production tools, such as those used in the microelectronic industry. The presently dominating procedure consists of the so-called *generic vibration criteria curves*, or simply VC curves. These curves are generic in the sense that they are intended to apply to broadly defined classes of equipment and processes (Gordon 91). Originally, each vibration class was defined in terms of a constant velocity (RMS) within the 8-80 Hz frequency range. These curves are characterized by:

- The velocity indicator expresses the vibration levels. The velocity indicator, as opposed to acceleration or displacement, is justified by the fact that, while different tools may exhibit increased sensitivity at different frequencies (internal natural frequencies), these points of increased sensitivity usually lie along a constant velocity curve (Gordon 91).

- The velocity is taken by the RMS (root-mean-square) representation, as opposed to instantaneous values (peak-to-peak, 0-to-peak, etc.). This energy-averaged representation provides a more appropriate description of how a tool will respond to the base excitation and, additionally, partly overcomes the consequence of finite record durations.
- The RMS velocity values are computed within proportional bandwidths. Actually, a one-third-octave bandwidth spectrum is recommended. This procedure implies that, at each frequency range, the frequency bandwidth is 23% of the centre frequency.
- For a site to comply with a particular vibration category, the corresponding one-third-octave band velocity spectra (in all three orthogonal directions) must lie below the appropriate VC curve.

The vibration criterion curves as proposed by Colin Gordon (Gordon 91) are illustrated in figure 2.

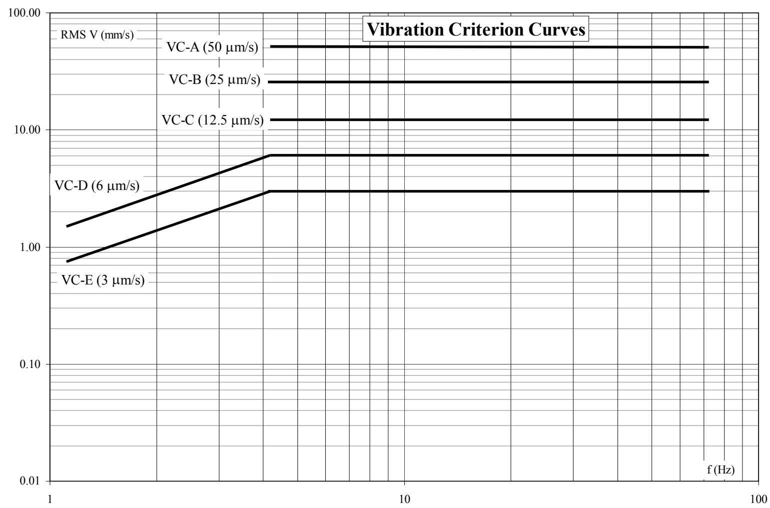

Figure 2. *Vibration Criterion (VC) curves (Gordon 1991)*

As shown, the 5 vibration criterion curves correspond to constant RMS velocity along most of the frequency range. However, in the low-frequency range the curves VC-D and VC-E are characterized by a constant displacement, in contrast with a constant velocity. RMS velocity spectrum is computed at the following centre frequencies: 4 Hz; 5.04 Hz; 6.35 Hz; 8 Hz; 10.08 Hz; 12.70 Hz; 16 Hz; 20.16 Hz; 25.40 Hz; 32 Hz; 40.32 Hz; 50.80 Hz; 64 Hz; 80.63 Hz. In some particular cases, the frequency band may be extended down to 2 Hz, which results in the additional centre frequencies of 2 Hz, 2.52 Hz and 3.17 Hz. Each tool should comply with a determinate VC class according to its dynamic stability requirements. For example, optical microscopes to 400X fit into VC-A, whereas electron microscope to 1 μm detail size should comply with VC-C.

2.3.3 *Mechanical Vibration Effects on Structural Components*

The effects of mechanical vibrations in structures can be subdivided according to the vibration sources or to the structural elements whose integrity is questioned. The vibration sources in structures can be external (in which the vibration is generally ground-borne) or internal (machinery operating within the structure). Applicable standards consider differently the integrity assessment of a specific structural component or of the structure as a whole. Generally speaking, the integrity of a specific structural component is questioned in situations where internal vibration sources prevail, whereas the overall integrity of the structure is addressed whenever the vibration source is external.

2.3.3.1 Overall integrity of the structure (external sources)

In the case of external sources – such as blasting, pile-driving, traffic and outside machinery – Portuguese Standard, NP-2074 (IPQ 1983) has been considered. This Portuguese standard, which generally conforms to other international standards (e. g.: DIN 4150-3, DIN 86), requires the measurement, at the foundation level, of triaxial velocity records under extreme events. The maximum measured velocity is then compared with permissible velocity levels, which, in turn, depend on the soil conditions, daily frequency of events and building importance. These permissible velocity levels were defined mostly by empirical observation of vibration effects on structures caused by external sources. The application of this standard is relatively straightforward, thus requiring no specific analytical background.

2.3.3.2 Integrity of a specific structural component (internal sources)

In the case of internal sources and apart from the analytical simulation of the as-measured, or predicted, excitation, most standards (e. g.: DIN 4150-3, DIN 86, and ISO 4866, ISO 90) refer to the estimation of the peak stress from the measured peak particle velocity for floor elements (beams and slabs/plates). To understand the underlying hypotheses, let us assume that the particular floor element vibrates at its natural frequency p (which corresponds to a modal shape described by $\psi(x)$). Consequently, the transverse deflection at the instant t – $q(x,t)$ – can be decomposed into a time-invariant component ($\overline{q}\,\psi(x)$, where $\psi(x)$ is the modal shape function and $\overline{q}$ its general amplitude) and a spatially invariant component (*sin(pt)*), as shown in figure 3.

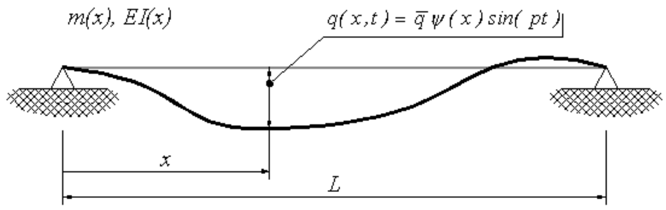

Figure 3. *Vibration shape for a given floor element*

Variables *m* and *EI* represent the vibrating unitary mass (mass per unit length) and flexural stiffness of the floor element.

The maximum deflection shape is, therefore, given by $q_{max}(x)=\overline{q}\,\psi(x)$ and the maximum deflection q_{max} is attained at a cross section $x=x_0$ in which the former equation attains its maximum value ($q_{max}=\overline{q}\,\psi(x_0)$).

The maximum kinetic energy follows:

$$C_{max}=\frac{m\,\overline{q}\,p^2}{2}\int_0^L \psi(x)^2\,dx \qquad [13]$$

Let us further assume that the curvature shape function ($\psi''(x)$, second derivative of the deflection shape function with respect to x) can be considered proportional to the deflection (α is the proportionality factor),

$$\psi''(x)=\alpha\,\psi(x) \qquad [14]$$

Under the former conditions, and considering only the flexural component, the maximum potential energy is expressed by:

$$V_{max}=\frac{EI\,\overline{q}^2\,\alpha^2}{2}\int_0^L \psi(x)^2\,dx \qquad [15]$$

The energy conservation principle shows that the kinetic and potential energy maxima are equal, from which results that the proportionality factor α is given by:

$$\alpha=p\sqrt{\frac{m}{EI}} \qquad [16]$$

The maximum velocity v_{max}, given by the following equation, is attained at the cross section of maximum deflection.

$$v_{max} = p\, q_{max} = p\, \bar{q}\, \psi(x_0) \qquad [17]$$

The former equation allows for the expression of the modal shape function maximum in terms of the (measured) velocity

$$\psi(x_0) = \frac{v_{max}}{p\, \bar{q}} \qquad [18]$$

The maximum curvature χ_{max} is also attained at the cross section of maximum deflection:

$$\chi_{max} = \bar{q}\, \alpha\, \psi(x_0) = v_{max} \sqrt{\frac{m}{EI}} \qquad [19]$$

to which corresponds the maximum stress (y, distance of the farthest fibre from the cross section centre of mass, and E, Young modulus),

$$\sigma_{max} = \chi_{max}\, y\, E = v_{max} \sqrt{\frac{m}{EI}}\, y\, E \qquad [20]$$

The former equation allows for the computation of the maximum stress directly from the measured velocity in the maximum deflection cross section.

For the specific case of a rectangular cross section, equation [20] leads to

$$\sigma_{max} = v_{max} \sqrt{E\, \rho}\, \sqrt{3\beta} \qquad [21]$$

where ρ and β respectively represent the mass density of the structural material, and a coefficient computed as the ratio between the total (structural and non-structural) mass and the structural mass alone. This equation is very similar to those presented both in DIN 4150-3 (DIN 1986) and ISO 4866 (ISO 1990), with the difference that both of these latter standards have an extra multiplying factor that accounts both for mode order effects and for boundary conditions.

3. Modal Identification Studies

3.1 The International Bridge in Vila Real de Santo António

This cable-stayed bridge over Guadiana river in the South of Portugal has a 324 m main span, two 135 m side spans, a monocellular prestressed deck and two, A-shaped, masts. Reception tests performed in August of 1992, considered some modal identification studies that were aimed at the validation of the numerical models used at the design stage, and at the establishment of a structural database for reference use in later tests.

ICIST/IST (Branco *et al.*, 1991), jointly with LNEC, was responsible for the modal identification stages of the superstructure as well as of the cables. Vibration records were collected in the vertical, transversal and longitudinal directions in the mid and quarter cross sections of the central span, as well as in some of the cables. While the majority of the vibration records are ambient, some of these were obtained as a consequence of transient, uncontrolled, vibrations which were imparted to the structure by means of: (1) travel of one, and two, heavily loaded 380 kN trucks; and (2) human-induced vibrations.

3.1.1 *Cable Frequencies*

The vibrating wire theory shows that, under some simplifying assumptions, the fundamental frequency f_1 of a vibrating wire relates to its length (L), unitary mass (m) and tensile force (F) by means of:

$$f_1 = \frac{1}{2L}\sqrt{\frac{F}{m}} \qquad [22]$$

The remaining, higher, mode frequencies are integer multiples of the fundamental frequency, as described in the former equation. These analytical results are the basis for the experimental measurement of the tensile force in cable elements, given their unitary mass and length.

In the specific bridge under study, ambient vibration records were collected with accelerometers transversally attached to some of the cables, next to their anchorage in the deck. Figures 4 and 5 represent the time and frequency domain counterpart for one of the instrumented cables.

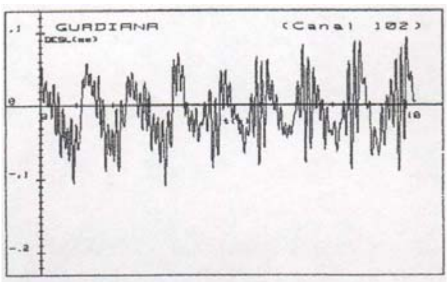

Figure 4. *Time domain record*

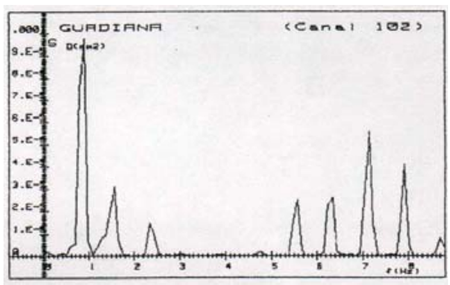

Figure 5. *Frequency domain counterpart*

Figure 5 clearly shows that the cable presents evenly spaced natural frequencies, as expected from the vibrating wire theory.

The experimentally measured fundamental frequency, and frequency spacing, allowed for the computation of the tensile force in each of the instrumented cables, given their length and unitary mass. These computed tensile force values match the results predicted by the numerical model used in design, as shown in table A.

Table A: Numerical *versus* Experimental cable frequencies

Cable	Force	L	m	Numerical	Experimental	
				Δf	Δf North	Δf South
	kN	m	kN m^{-2} s^2	Hz	Hz	Hz
1	4817	170.2	0.073	0.76	0.78	0.78
3	3086	152.2	0.05	0.82	0.85	0.85
5	2871	134.6	0.05	0.89	0.9	0.9
7	2736	117.4	0.05	1.00	1.03	1.02
9	2417	100.4	0.041	1.21	1.27	1.25
11	2092	84.1	0.033	1.49	1.55	1.52
13	1727	68.9	0.029	1.77	1.9	1.9
15	1363	55.5	0.029	1.95	2.1	2.15

3.1.2 *Deck Frequencies*

Numerical models used in design had shown that the mode shape frequencies cluster heavily (e.g. there were in excess of 30 mode shapes with frequencies below 3 Hz). On the other hand, ambient vibration records collected in the deck in the vicinity of the cables showed that the motion of the deck is to some extent influenced by the vibration of the nearby cables.

Deck frequencies were experimentally determined though the collection of ambient vibration acceleration records at different cross sections (mid span, quarter span, etc.) and at different locations in each of these cross sections (North, upstream, centre and South, downstream). The correspondent individual spectral estimates for each of these (so-called *direct*) records, were consequently computed. The so-called *indirect* records were also computed in the time domain (e.g. semi-sum and semi-subtraction of synchronous vertical records collected at the upstream and downstream locations for a determinate cross section), and the correspondent spectral estimates were computed. Figures 6 and 7 exemplify some of the results pertaining to the mid span cross section of the deck.

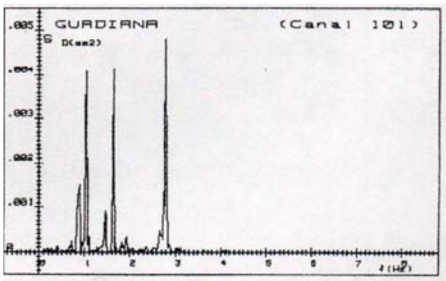

Figure 6. *Indirect record (sum)*

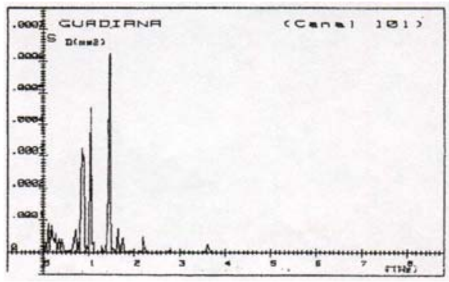

Figure 7. *Indirect record (subtraction)*

The observation of example figures 6 and 7 show that:

- peaks existent in figure 6 in frequencies 1.64 and 2.78 Hz correspond to flexural mode shapes;
- peaks at frequencies 0.85, 1.04 and 1.45 Hz correspond to combined flexural-torsional mode shapes;
- no exclusively torsional mode shapes were identified.

3.2 Precast Bench Elements at Sporting Clube de Portugal New Lisbon Stadium

SCP (Sporting Clube de Portugal), has just finished in 2003 the construction of the new, Alvalade XXI, football stadium that will host some of the games of the Euro 2004 championship. One of the stadium's most distinguishing features consists in the extensive use of the precast and prestressed RC bench elements. These elements are relatively slender, reaching lengths of 12 m. The predicted, single element vertical motion natural frequencies – disregarding the connection between every two superimposed bench elements and other stiffening effects – were in the order of 5 to 6 Hz. These values are considerably lower than the minimum frequency values prescribed either in Eurocode 1 (CEN 2000) and CEB (CEB 1991) to preclude the explicit verification of the effects of the rhythmical and synchronised movement of crowds. This problem was further made worse by the fact that the manufacturing process, in which the bench elements were cast in an inverted position, led to the development of evenly distributed cracks when the prestressing force was applied.

The uncertainties about the dynamic properties of the bench elements led to modal identification tests, carried both in the factory (with a single bench element) and in the stadium, upon placement and interconnection between superimposed elements.

3.2.2 *Modal Identification Tests Carried Out in Factory*

Tests carried out in factory (Proença *et al.*, 2001.2) were conducted on a single specimen with a total length of 10.5 m (8.85 m between support axes) in the following three different successive stages:

- Preliminary modal identification without additional loads.
- Modal identification with an additional mid span load. A concrete block was suspended at mid span so that the corresponding bending moment increase at the same cross section was 41% of the design bending moment due to live loads.
- Final modal identification without additional loads (after the release of the additional mass).

Figures 8 and 9 represent the cross section of the tested specimen and the suspended concrete block during the releasing stage.

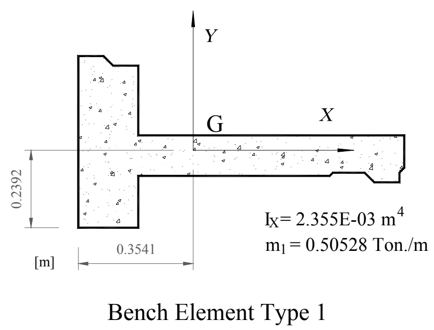

Figure 8. *Cross section of the bench*

Figure 9. *Concrete block and bench*

The experimental tests consisted in the measurement of the mid span vertical acceleration under the three referred different stage load conditions. Figure 10 shows the time history response during the release of the suspended concrete block.

Data processing consisted in the identification of the fundamental frequencies, and correspondent modal damping ratios, for the same three stages. Figure 11 summarizes the normalized power spectral densities for records collected in the first (CG001 and CI001), second (CJ002 and CJ003) and third (CJ005) stages.

The estimated fundamental frequency values were within the 6.64-7.03 Hz range for the first and third stages (without additional loads) and around 5.86 Hz for the second stage (with the suspended concrete block). The fact that first and third stage frequency values are similar indicates that there is full recovery of the original stiffness after the release of the suspended concrete block. The fundamental frequency value for the second stage is lowered as a consequence of the extra mass provided by the concrete block. The frequency resolution for these power spectral densities (0.195 Hz) is relatively coarse as a consequence of the oversampling process used in the PSD (Power Spectral Density) estimation for these records.

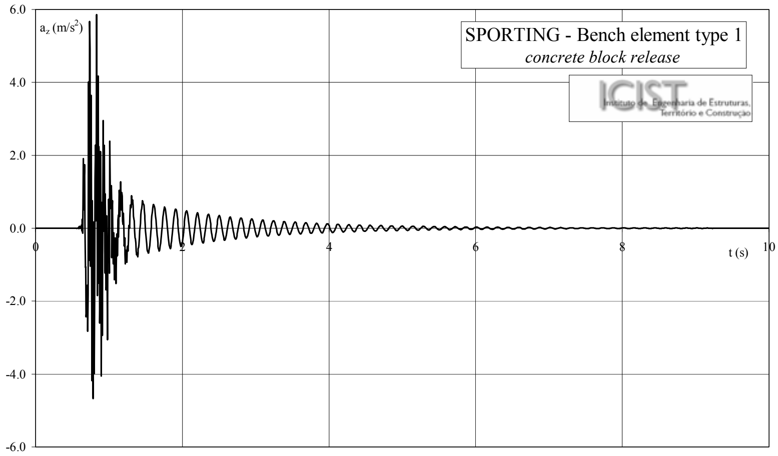

Figure 10. *Free vibration response during the suspended concrete block release*

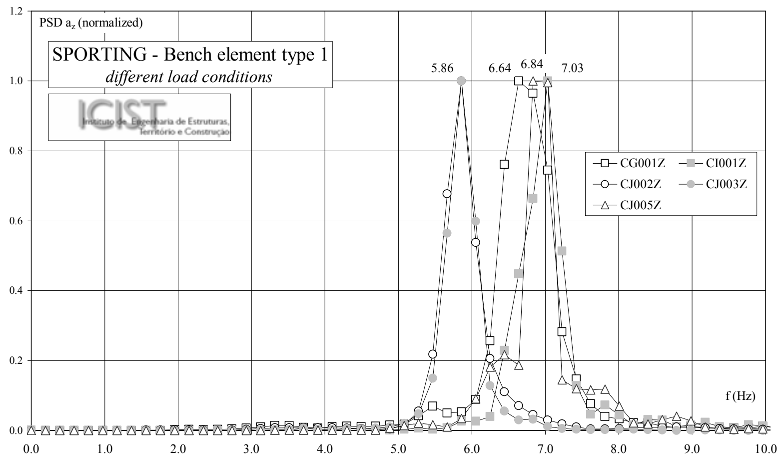

Figure 11. *Normalized power spectrum densities for all stages*

Figure 12 shows the result of curve fitting equation [8] to experimental data referring to the free vibration decay time segment, immediately after the release of concrete block. The estimated fundamental frequency and viscous damping ratio were, respectively, of 6.75 Hz and 1.79%.

Subsequent analytical modelling showed that cracking induced by the manufacturing process had no measurable detrimental effect on the stiffness of the bench elements, and, moreover, that the extra mass effect was the sole responsible for the decrease of frequency in the second stage tests.

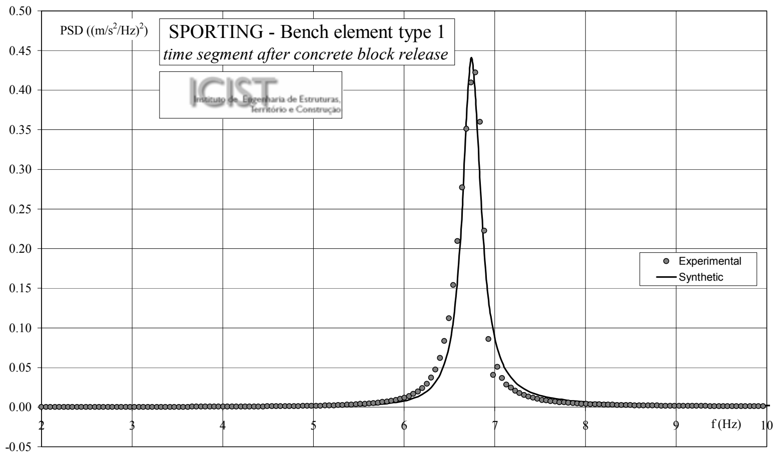

Figure 12. *Curve fitting results for free vibration time segment*

Even tough the tests conducted in the factory were generally favourable, a final recommendation was made to increase the unified behaviour of every two superimposed bench elements. This recommendation further stressed the need for grouting the correspondent horizontal joints, as well as for the inclusion of steel dowels placed at the mid span cross section in-between some of the superimposed bench elements.

3.2.3 *Modal Identification Tests Carried Out in the Stadium*

Tests performed after the completion of the stadium's structure included modal identification of four of the most representative bench elements (Proença 2003). Generically speaking, the most important differences presented by these elements were the cross section shape and the length, which varies almost continuously as a consequence of the enlargement of the stands with the increase of the distance to the field. There were two main cross section types, respectively in the lower stand (element type 1) and higher stand (element type 2).

Excitation consisted in ambient vibration or human jumps, either in the tested or in the adjoining bench elements. Preliminary observation of the time domain vibration records showed that there was an effective interaction between superimposed bench elements, as excitation applied several rows apart caused distinct and synchronized motion in the instrumented elements.

The tested benches were two of element type 1 (lower stand) and other two of element type 2 (higher stand).

Modal testing was aimed at the identification of the fundamental vertical vibration frequencies and corresponding viscous damping ratios. Figure 13 exemplifies the comparison of raw data PSD and curve fitted curves according to equation [8].

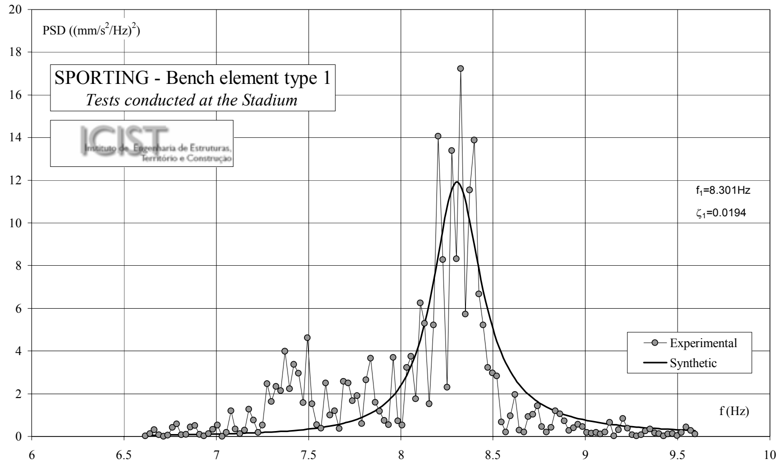

Figure 13. *Example of curve fitting results for bench element type 1*

The fundamental frequency and viscous damping ratios were, respectively, of 8.301 Hz and 1.94%.

Table 1 summarizes the identified fundamental frequencies and viscous damping ratios for the four tested representative bench elements.

Bench Element	Length	Stand	f_1 Hz	ζ_1 %
Type 1	shorter	lower	10.8	2.4
Type 1	longer	lower	8.3	1.9
Type 2	shorter	higher	9.5	1.7
Type 2	longer	higher	7.6	2.2

Table 1. *Summary of the identified modal properties*

3.3 Santa Maria Hospital Complex

The Santa Maria Hospital building complex (aerial view and plan respectively shown in figures 14 and 15) consists of 47 cast-in-situ reinforced concrete frame building blocks, 1 to 11 storeys high, separated by expansion joints. This Hospital has a total area of 120 000 m^2, presently with over 1000 internment beds, being situated in Lisbon, within the Portuguese highest seismic risk zone. The building design and construction started in the late 1930s and ended in 1953, before earthquake-resistant design clauses were included in the Portuguese structural design codes.

Figure 14. *Santa Maria Hospital Complex (aerial view)*

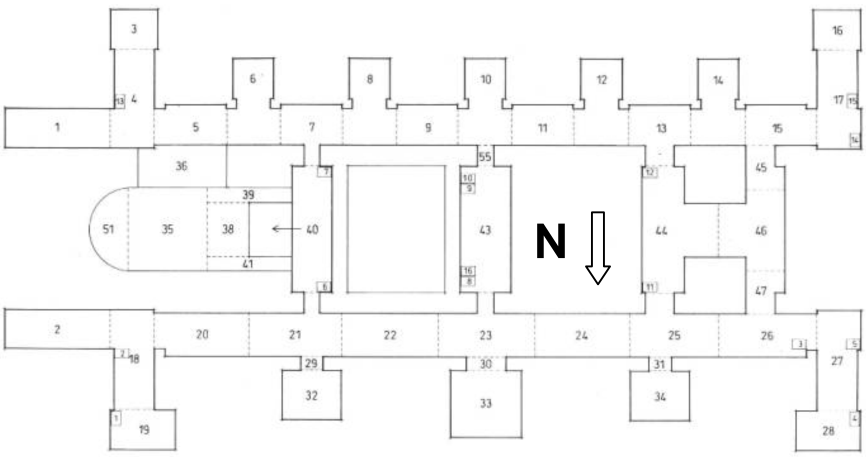

Figure 15. *Santa Maria Hospital Complex (plan)*

Considering the uncertain seismic behaviour and the extreme importance of this health care unit, the Portuguese Health Ministry asked ICIST/IST for the seismic vulnerability assessment of the hospital structure (Oliveira *et al.*, 2003).

The lateral load structural behaviour of the building blocks is highly dependent on the effectiveness of the separation joints, as well as on the stiffness and strength contribution of the masonry wall panels. Considering these uncertainties and prior to the development of refined numerical models, the modal identification stages were undertaken. These stages comprised the *simplified modal identification* of fourteen different building blocks and the *complete modal identification* of building block #4 (one of the corner building blocks, with a 150 m^3 water tank on roof). *Simplified modal identification* is aimed only at the identification of the fundamental frequencies, which can be accomplished by the collection of ambient vibration records at a single storey, generally the highest one. *Complete modal identification* is aimed at the identification of modal frequencies and modal shapes of a given building structure, requiring intensive and lengthy instrumentation of all building storeys and the collection of synchronized ambient vibration records.

Figure 16 depicts the normalized Y-direction (N-S) acceleration power spectra for ambient vibration records collected in building blocks #8, 9, 10, 16, 17 and 43.

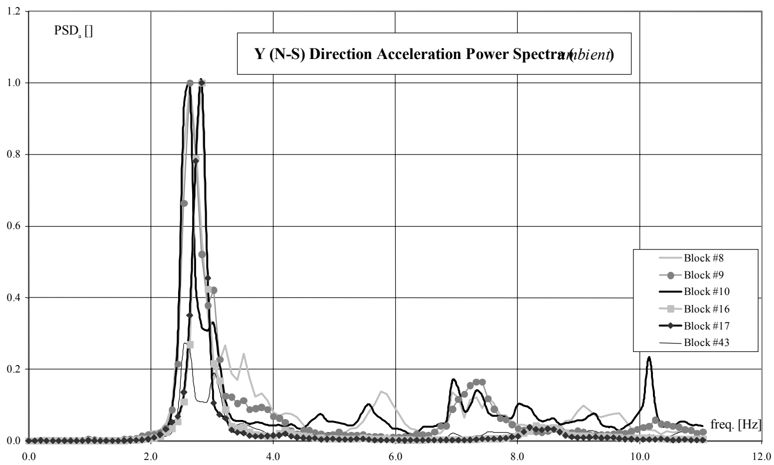

Figure 16. *Normalized ambient vibration acceleration power spectrum for building blocks #8, 9, 10, 16, 17 and 43 (Y - N-S direction).*

Simplified modal identification results, exemplified in figure 16, clearly point out to a unified behaviour of the building blocks, with a fundamental frequency value of 2.4-2.8 Hz for X (E-W) direction and 2.4-2.8 Hz for Y (N-S) direction. This unified behaviour has been attributed to the fact that the joints are not working properly. Experimentally determined modal frequency values are twice to three times those conveyed by bare frame RC numerical models. This discrepancy clearly stresses the stiffening effect of the masonry walls, generally disregarded at the numerical modelling level.

Complete modal identification of building block #4 was performed according to the BFD (see equation [9]). Figure 17 depicts the lower order mode shapes in the X (E-W) and Y (N-S) directions for building block #4.

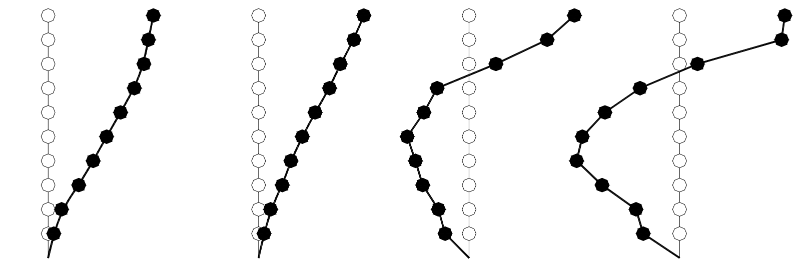

Figure 17. *Lower order mode shapes for building block #4*

The experimentally determined mode shapes show that the maximum inter-storey drift occurs within intermediate storeys, leading to higher demands on the (RC and masonry) elements in-between these storeys. This observation was later confirmed at the non-linear modelling stage, where an incipient intermediate soft-storey was found to develop as a consequence of the crushing of all masonry wall elements existent at that intermediate storey.

4. Mechanical Vibration Characterization Studies

4.1 Vibration Measurements and Qualification for Semiconductor Fabrication Facilities in Northern Portugal

In 2001, ICIST/IST (Proença *et al.*, 2001.1) was asked to perform ambient vibration site qualification in three different sites for the possible construction of a semiconductor production facility in Northern Portugal. These sites will hereafter be identified by their locations: *Castelões*, *Modivas* and *Laundos*.

The qualification of each site was performed in accordance with the generic vibration criterion curves – previously referred to as *VC curves* – as proposed by

M+Zander Facility Engineering GmbH (Germany) and Angelou Economic Advisors, Inc. (USA). These curves were comparable to the ATF (Advanced Technology Facility) industry standards, as set by IEST – Institute of Environmental Sciences and Technology (IEST 93).

Vibration measurements were made considering the vibration sources characteristics of each site. These vibration sources included: road traffic (cars and trucks) along IC1 (a nearby freeway); heavy trucks traffic along adjoining secondary roads; train passages (in only one of the sites); and other, site-dependent, activities that induced vibrations in the selected building sites.

In situ vibration measurement consisted in the collection of triaxial acceleration records, with individual durations between 100 s and 130 s, and sampling rates of 250 Hz. Sub-superficial vibrations characterization was performed in specifically dug trenches (6, 4 and 6, respectively in locations Castelões, Modivas and Laundos). These records were obtained for the following set of differentiating factors:

- Location – a group of records (between 4 and 6) was obtained per trench in all of the 16 designated trenches.
- Depth – part of the records was collected at the surface – within the vicinity of the designated trench – and the remaining part was collected in depth (just above the ground water table or close to the bottom of the trench).
- Vibration source – in those trenches where the vibration source could be clearly identified, vibration records were collected individuating the different vibration sources.

For the majority of the trenches, a set of two records was collected in depth and another set of two records was collected at the surface. Whenever the vibration source could be identified, a group of additional records were collected.

When useful, records were cropped in the time domain, in order to emphasize a specific vibration source.

The main objective of the data processing stages consisted in the plot of the RMS velocity spectra for the group of one-third-octave frequency bands, from which the compliance with the different VC classes could be checked for both superficial and in-depth vibration records. Different RMS velocity spectra were then obtained for each of the orthogonal components (two in the horizontal plane and a third in the vertical direction) and for each of the records. Before the RMS velocity spectra was computed, the large majority of the records were digitally filtered by a 6th order Butterworth high-pass filter at 1 Hz to eliminate any, spurious, DC or near DC drift components.

Global results can be exemplified by figure 18, which shows maxima results for one of the trenches dug in Castelões. The RMS velocity spectra, shown for the group of one-third-octave frequency bands, were computed combining the maxima for all directions and for all records made at a given depth (and distance to the freeway).

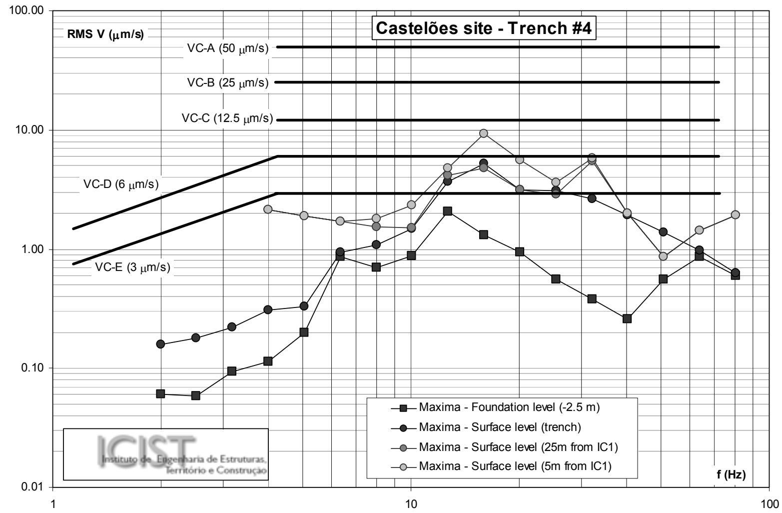

Figure 18. *Global results for trench T4 (Castelões)*

Vibration traces for records obtained in trench T4 and in its vicinity with varying distances to the major vibration source – the IC1 speedway – show that the vibration levels only comply with VC class E in the in-depth records, whereas all superficial records (near the trench, 25 m from the IC1 and 5 m from the IC1) would lead to VC classes D or C. The decrease of the distance to the IC1 speedway clearly leads to an overall increase of the vibration levels in inverse correlation with the former distance.

Similar results not shown were obtained for the remaining trenches and remaining sites, leading to the qualification of these sites and, moreover, of the most favourable areas within each of these three sites.

4.2 Vibration Measurement in a Fertilizer Production Plant, near Setúbal

In 2000 ICIST/IST (Proença *et al.*, 2000) was asked to characterize existent mechanical vibrations and propose remedial solutions for the new grinding area of an existent fertilizer production complex, near Setúbal. The new grinding area comprises two adjoining buildings, as shown in figure 19. One of these buildings – the office building – housed electrical distribution boards in the first storey and had a control room (with PCs and other electrical equipment) in the second storey. The second building housed the two major vibration sources: the drier, which rested directly on the ground; and the grinder, which was placed at the same level of the control room.

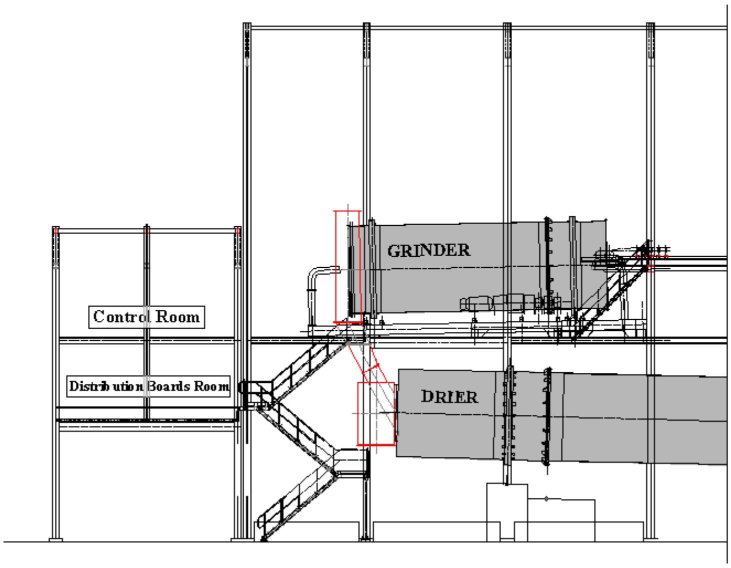

Figure 19. *Cross section of the new grinding area unit*

The main complaints referred to excessive vibrations felt at the control room, both in terms of comfort and of the integrity of the equipment, as well as of possible damage to the underlying electrical distribution boards.

Vibration characterization tasks evolved in two different stages: one first, preliminary, stage, in which vibration measurements were made at different locations; and a second stage, after some structural modifications, which tried to assess the alleged benefits. In both stages, vibration characterization was performed considering human health and comfort issues, possible damage to equipment and possible damage to the structure.

Amongst other objectives, first stage measurements were intended to identify the most influencing vibration source – the grinder or the drier – as well as the dependence on the load conditions (both of these two equipments could operate under reduced or full load conditions). This was accomplished through the identification of the so-called *spectral signatures* of both equipments, as well as through measurements made under different operating conditions (the drier alone, the grinder alone, both operating simultaneously, different load conditions, etc.). Figure 20 summarizes X-direction (horizontal direction of figure 19) acceleration PSD traces for different records collected under these different load conditions in one representative point in the control room.

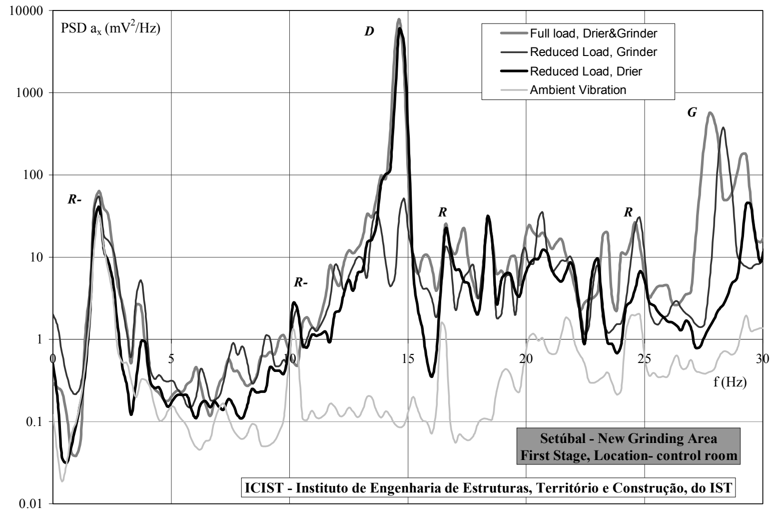

Figure 20. *PSD X-direction trace comparison (fist stage, control room)*

Peaks existent in figure 20 were identified by marks R- (structural peak, no resonance), R (structural peak, resonance), D (drier operation peak) and G (grinder operation peak). These results show that fundamental X-direction mode shape frequency is in the range from 1.93 Hz to 2.4 Hz, and, moreover, that the different operating conditions seem to have no effect on its magnitude. Mode shape with frequency of 16.5 Hz is, however, excited by both the grinder and, specially, the drier operation. Peaks in the vicinity of 14.7 Hz are dominant and clearly result from the drier operation, independently of its load. Grinder operation is responsible for peaks in the range from 27 Hz to 28 Hz, dependent on the operating load conditions.

Former results point to the drier operation as the main cause for the vibrations felt on the control room. Vibration is transmitted through the ground, on which the drier is placed, to the office structure foundations, and then transmitted upwards through the structural elements. One of the structural modifications consisted in the isolation of the vibrations transmitted at the foundation of the drier, which was accomplished by the excavation of trenches around these elements and placement of isolation mats. Another structural modification consisted in the separation of the footings of the two adjoining structures (a common footing served as direct foundation element for the columns of these two structures).

Vibration qualification in the control room (the only location where operator permanence was expected) showed that KB values were of 0.9 mm/s (horizontal direction) and 6.5 mm/s (vertical direction). The limiting values are 0.4/0.6 mm/s (day/night shift) for industrial facilities and continuous vibrations, as prescribed by DIN 4150 (part 2). Vertical amplification was attributed to floor excessive flexibility and possible resonance.

Structural integrity was assessed through the indirect computation of the maximum stress at the midspan of the beams near the grinder though equations [20] and [21]. The results show that cyclic stresses induced by the operation of this equipment are lower that 5 MPa, posing no problem to structural integrity.

Possible damage to electronic equipment led to the computation of RMS velocity spectra for the group of one-third-octave frequency bands, from which the compliance with the different VC classes could be checked.

5. Conclusions

Developments in the sensor technology, through the supply of adapted vibration transducers (low level vibration, high level/shock vibration, near-static sensitivity, etc.), in conjunction with the dissemination of digital processing algorithms, has lead to a notable increase in the study of mechanical vibrations in structures. Applications range from modal identification (either simplified or complete) to the characterization of vibrations problems. These problems are related to human health and comfort issues, and possible damage to structures (and structural components) and to sensitive equipments.

Modal identification in civil engineering structures has generally been performed according to the Basic Frequency Domain (BFD) method, and has typically led to the refinement and validation of analytical or numerical models, as well as to damage assessment of structures and structural components.

Vibration effects on human health and comfort can be expressed in terms of the human perceptibility factor KB, as defined by DIN 4150-2 (DIN 1975) and DIN 45669 (DIN 1995). Vibration effects on sensitive equipment can be expressed in terms of RMS velocity one-third octave frequency band spectra, as suggested in the standards for advanced technology facilities. Vibration effects on structures as a whole, when external vibration sources prevail, require the measurement of vibrations (velocity) under extreme events at the foundation level. Vibration effects on structural components induced by internal sources, namely in floor components (slab and beam elements) with generic cross-sections can be assessed though the indirect computation of cyclic stress maxima, as defined by equation [20].

6. References

Bendat J. S., Piersol A. G. *Engineering Applications of Correlation and Spectral Analysis*, New York, Wiley, 2000.

Branco F., Proença J. M., Azevedo J. J., *Ensaios Dinâmicos na Ponte do Guadiana em Vila Real de Santo António* (Dynamic Tests on the over Guadiana River Bridge in Vila Real de Santo António), Internal Report CMEST (former ICIST) EP Nº 35/91, 1991, CMEST/IST.

CEB, *Vibration Problems in Structures. Practical guidelines.*, CEB – Comité Euro-International du Beton, Lausanne, 1991.

CEN, CEN/TC250/SC1, *Draft prEN 1991-1-1: EUROCODE 1 - Actions on structures. Part 1.1: General Actions -Densities, self-weight, and imposed loads*, CEN, 2000.

DIN, Deutsches Institut für Normung (German Standards Organization), Vibrations in Building Construction. Part 2 - Influence on people on buildings. DIN 4150-2, Berlin 1975.

DIN, Deutsches Institut für Normung (German Standards Organization), Vibrations in Building Construction. Part 3 – Effects on structures. DIN 4150-3, Berlin 1986.

DIN, Deutsches Institut für Normung (German Standards Organization), Mechanical Vibration and Shock Measurement. Part 1 – Measuring equipment. DIN 45669-1, Berlin 1995.

Ewins D. J., *Modal Testing: Theory and Practice*, John Wiley and Sons, 1986.

Gordon Colin G., “Generic Criteria for Vibration-Sensitive Equipment”, *SPIE Proceedings,* Volume 1619, 1991.

IEST, Considerations in Cleanroom Design, report RR-CC012.1, ISET - Institute of Environmental Sciences and Technology, 1993.

IPQ, Instituto Português da Qualidade (Portuguese Institute for Quality), Evaluation of the influence on constructions of vibrations induced by blasting or similar events, NP-2074, Lisbon 1983.

ISO, International Standards Organization, Mechanical Vibration and Shock – Vibration of buildings – Guidelines for the measurement of vibrations and evaluation of their effects on buildings, ISO 4866, Genève, 1990.

Oliveira C. S., Proença J. M., Almeida J. P., Ferreira P., *Programa de Avaliação da Vulnerabilidade Sísmica das Instalações Hospitalares da Área Metropolitana de Lisboa. Estudo-Piloto do Hospital de Santa Maria*. (Seismic Vulnerability Assessment Programme for Healthcare Facilities in the Greater Lisbon Metropolitan Area. Pilot-study of the Santa Maria Hospital), Internal Report ICIST EP Nº 25/03, 2003, ICIST/IST.

Proença J. M., Oliveira C. S., *Caracterização das Vibrações Mecânicas na Área de Granulação IV da Fábrica de Adubos da SAPEC, em Setúbal. Recomendações para a sua atenuação*. (Mechanical Vibrations Characterization in the Grinding

Area IV of SAPEC's Fertilizer Plant, in Setubal. Attenuation recommendations.), Internal Report ICIST EP Nº 40/00, 2000, ICIST/IST.

Proença J. M.; Azevedo J. J., Vibration Measurement and Qualification of Three Possible Semiconductor Fabrication Facilities in Northern Portugal, Internal Report ICIST EP Nº 2/01, 2001, ICIST/IST.

Proença J. M.; Lúcio V., *Identificação de Frequência Fundamental em Bancada da Soplacas* (Fundamental Frequency Identification in Soplacas' Bench), Internal Report ICIST EP Nº 79/01, 2001, ICIST/IST.

Proença J. M., *Identificação das Frequências Fundamentais em Elementos Pré-fabricados de Bancada do Novo Estádio do Sporting Clube de Portugal* (Fundamental Frequency Identification for Precast Bench Elements of the New Stadium of the Sporting Clube de Portugal), Internal Report ICIST EP Nº 45/03, 2003, ICIST/IST.

Ventura C., "Identification by the Basic Frequency Domain (BFD) Technique", *Modal Identification of Output-Only Systems*, Course Notes, Madrid, 2000.